All-Fiber Photon-Pair Source for Quantum Communications

Marco Fiorentino, Paul L. Voss, Jay E. Sharping, and Prem Kumar

***Abstract*—In this letter, we present a source of quantum-correlated photon pairs based on parametric fluorescence in a fiber Sagnac loop. The photon pairs are generated in the 1550-nm fiber-optic communication band and detected with InGaAs–InP avalanche photodiodes operating in a gated Geiger mode. A generation rate $> 10^3$ pairs/s is observed, which is limited by the detection electronics at present. We also demonstrate the nonclassical nature of the photon correlations in the pairs. This source, given its spectral properties and robustness, is well suited for use in fiber-optic quantum communication and cryptography networks.**

***Index Terms*—Fiber four-wave mixing, parametric amplifiers, photon counting, quantum communication, quantum cryptography.**

EFFICIENT generation and transmission of quantum-correlated photon pairs, especially in the 1550-nm fiber-optic communication band, is of paramount importance for practical realization of the quantum communication and cryptography protocols [1]. The workhorse source employed in all implementations, thus far [2] has been based on the process of spontaneous parametric down-conversion in second-order [$\chi^{(2)}$] nonlinear crystals. Such a source, however, is not compatible with optical fibers as large coupling losses occur when the pairs are launched into the fiber. This severely degrades the correlated photon-pair rate coupled into the fiber, since the rate depends quadratically on the coupling efficiency. From a practical standpoint, it would be advantageous if a photon-pair source could be developed that not only produces photons in the communication band but also can be spliced to standard telecommunication fibers with high efficiency. Over the past few years, various attempts have been made to develop more efficient photon-pair sources, but all have relied on the $\chi^{(2)}$ down-conversion process [3]–[6]. Of particular note is [4], in which the effective $\chi^{(2)}$ of periodically poled silica fibers was used. In this letter, we report the first, to the best of our knowledge, photon-pair source that is based on the Kerr nonlinearity ($\chi^{(3)}$) of standard fiber. Quantum-correlated photon pairs are observed and characterized in the parametric fluorescence of four-wave mixing (FWM) in dispersion-shifted fiber (DSF).

The FWM process takes place in a nonlinear-fiber Sagnac interferometer (NFSI), shown schematically in Fig. 1. Previously, we have used this NFSI to generate quantum-correlated twin beams in the fiber [7]. The NFSI consists of a fused-silica 50/50 fiber coupler spliced to 300 m of DSF having zero-dispersion wavelength $\lambda_0 = 1537$ nm. It can be set as a reflector with proper adjustment of the intraloop FPC to yield a transmission coefficient < -30 dB. When the injected pump wavelength is slightly greater than λ_0, FWM in the DSF is phase matched [8]. Two pump photons of frequency ω_p scatter into a signal photon and an idler photon of frequencies ω_s and ω_i, respectively, where $\omega_s + \omega_i = 2\omega_p$. Signal-idler separations of $\simeq$ 20 nm can be easily obtained with use of commercial DSF [7]. The pump is a mode-locked train of $\simeq$3-ps-long pulses that arrive at a 75.3-MHz repetition rate. The pulsed operation serves two important purposes: 1) the NFSI amplifier can be operated at low average powers (typical values are $\leq$ 2 mW, corresponding to $\leq$ 9 W peak powers) and 2) the production of the fluorescence photons is confined in well-defined temporal windows, allowing a gated detection scheme to be used to increase the signal-to-noise ratio. A 10% (90/10) coupler is employed to inject a weak signal, which is parametrically amplified and the output signal and the generated idler are used for alignment purposes. For the photon-counting measurements described in this letter, the input signal is blocked.

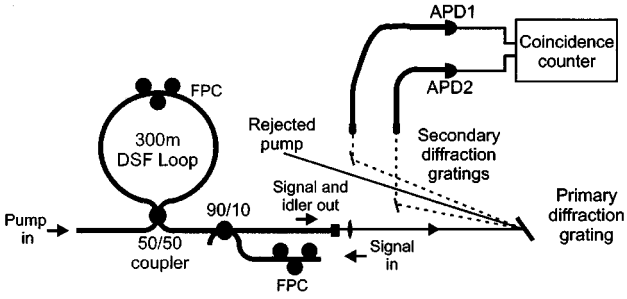

Fig. 1. Diagram of the experimental setup. FPC: Fiber polariziation controller.

After passing through the 90/10 coupler, the fluorescence photons are directed toward free-space filters that separate the signal and the idler photons from each other and from the pump photons. To measure the nonclassical (i.e., quantum) correlations between the signal and the idler photons, one must effectively suppress the pump photons from reaching the detectors. Since a typical pump pulse contains $\simeq 10^8$ photons and we are interested in detecting $\simeq$ 0.01 photons/pulse, a pump-to-signal (idler) rejection ratio in excess of 100 dB is required. To meet this specification, we constructed a dual-band spectral filter based on a double-grating spectrometer. A primary grating (holographic, 1200 lines/mm) is first employed to spatially separate the signal, the pump and the idler photons. Two

Manuscript received January 01, 2002; revised March 22, 2002. This work was supported in part by the DoD Multidisciplinary University Research Initiative (MURI) Program administered by the Army Research Office under Grant DAAD19-00-1-0177 and by the U.S. Office of Naval Research under Grant N00014-91-J-1268.

The authors are with the Center for Photonic Communication and Computing, ECE Dept., Northwestern University, Evanston, IL 60208 USA.

Publisher Item Identifier S 1041-1135(02)05302-8.

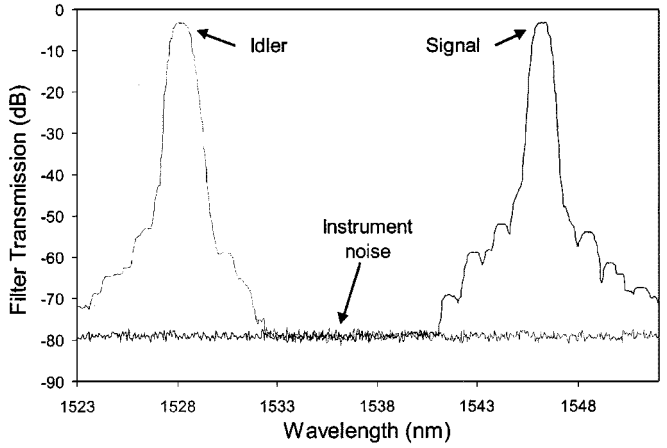

Fig. 2. Transmission curves of the signal and idler channels in the dual-band filter.

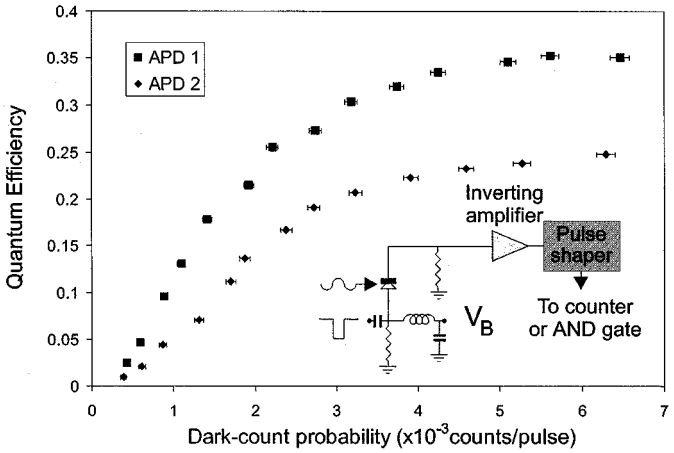

Fig. 3. Quantum efficiency versus dark-count probability for the two APDs used in the experiments. The inset shows a schematic of the electronic circuit used with the APDs.

secondary gratings (ruled, 600 lines/mm) are then used to prevent the pump photons that are randomly scattered by the primary grating (owing to its nonideal nature) from going toward the signal and idler directions. The doubly diffracted signal and idler photons are then recoupled into fibers, which function as the output slits of the spectrometer.

Transmission spectrum of the dual-band filter, measured with a tunable source and an optical spectrum analyzer (OSA), is shown in Fig. 2. The shape is Gaussian in the regions near the maxima of the two transmission bands, which are centered at 1546 nm (signal) and 1528 nm (idler), respectively, and the full-width at half-maximum (FWHM) is $\simeq 0.46$ nm. For pulse trains separated by 9 nm, which is the wavelength difference between the pump and the signal (or idler), this filter is able to provide an isolation $\geq$ 75 dB; the measurement being limited by the intrinsic noise of the OSA. The combined effect of the Sagnac loop and the double-grating filter, thus provides an isolation $\geq$ 105 dB from the pump photons in the signal and idler channels. The maximum transmission efficiency in the signal channel is 45% and that in the idler channel is 47%. The total collection efficiency for the signal (idler) photons is thus 33% (35%), with inclusion of the losses in the Sagnac loop (18%), and at the 90/10 coupler (10%).

The separated and filtered signal and idler photons are directed toward fiber-pigtailed InGaAS–InP avalanche photodiodes (APDs, Epitaxx EPM239BA). In recent years, the performance of InGaAs APDs as single-photon detectors for use in the fiber communication window around 1550 nm has been extensively studied by several groups [9]–[12]. The pulsed nature of the photon pairs allows us to use the APDs in a gated Geiger mode. In addition, the quality of our APDs permits room-temperature operation with results comparable to those obtained by other groups at cryogenic temperatures. A schematic of the electronic circuit used with the APDs is shown in the inset in Fig. 3. A bias voltage V_B ($\simeq -60$ V), slightly below the avalanche breakdown voltage, is applied to each diode and a short gate pulse (-8 V, 1-ns FWHM) brings the diodes into the breakdown region. The gate pulse is synchronized with the arrival of the signal and idler photons on the photodiodes. Due to limitations of our gate-pulse generator, the detectors are gated once every 128-pump pulses, giving a photon-pair detection rate of $75.3\ \text{MHz}/128 = 588$ kHz. We expect this rate to increase by more than an order of magnitude with use of a better pulse generator. The electrical signals produced by the APDs in response to the incoming photons (and dark events) are reshaped into 500-ns-wide TTL pulses that can be individually counted or sent to a TTL AND gate for coincidence counting.

In Fig. 3, we show a plot of the quantum efficiency versus the dark-count probability for the two APDs used in our experiments. A figure-of-merit for the APDs can be introduced through the noise-equivalent power NEP $= (h\nu/\eta)(2R_D)^{1/2}$ [9], where h is the Planck constant, ν is the frequency of light, η is the detector quantum efficiency, and R_D is the dark-count rate measured during the gate time. The best values of NEP obtained by optimizing V_B are 1.0×10^{-15} W $\cdot$ Hz$^{-1/2}$ for APD1 and 1.6×10^{-15}W $\cdot$ Hz$^{-1/2}$ for APD2. These values are comparable to those reported in [9]–[12] for cryogenically cooled APDs. Under the optimized conditions the efficiency of APD1 (APD2) is 25% (20%) and the corresponding dark-count probability is 2.2×10^{-3}/pulse (2.7×10^{-3}/pulse).

As a first test of our photon-pair source and of the filtering process, we measure the number of scattered photons detected in the signal (idler) channel N_S (N_I) as a function of the number of pump photons N_P injected into the NFSI. The results for the idler channel are shown in the inset in Fig. 4. We fit the experimental data with $N_S = N_D + s_1 N_P + s_2 N_P^2$, where N_D is the number of dark counts during the gate interval and s_1 and s_2 are the linear and quadratic scattering coefficients, respectively. The fit clearly shows that the quadratic scattering owing to FWM in the fiber can dominate over the residual linear scattering of the pump due to imperfect filtering.

In Fig. 4, we present the coincidence counting results. The diamonds represent the rate of coincidence counts as a function of the rate of the signal and idler photons generated during the same pump pulse. For convenience, we have plotted the coincidence rate as a function of the geometric mean of the signal and idler count rates. In fact, since the efficiency of the two detectors is different, we measure different single-photon count rates in the two channels. Dark counts have been subtracted from the

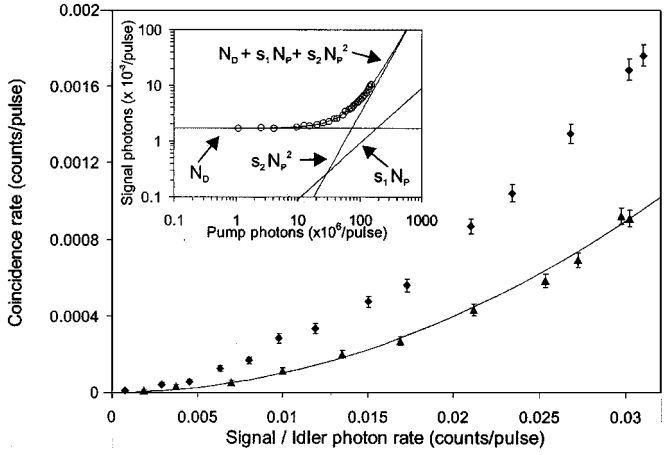

Fig. 4. Coincidence rates as a function the single-photon rates in two different cases. Signal-idler fluorescence produced by a pump pulse (diamonds) and signal-idler fluorescence produced by two consecutive pump pulses (triangles). The line represents the calculated "accidental" counts. The inset shows a plot of the detected idler photons as a function of the injected pump photons (hollow circles). A second-order polynomial is shown to fit the experimental data. The contributions of the dark counts, linear scattering and quadratic scattering are plotted separately as well.

plotted count rates. For the coincidence rates, both dark-dark and photon-dark coincidences have to be taken in account, but for the counting rates in our experiment the former are negligible. Thus far, we have achieved a maximum coincidence rate of 10^3 counts/s (= coincidence rate/pulse $\times$ gate-pulse rate), which is expected to go up by at least a factor of ten with use of a higher repetition-rate gate-pulse generator.

We have performed two independent experiments to demonstrate the nonclassical nature of the coincidences. Results of the first experiment are shown by the triangles in Fig. 4, which represent the measured coincidence rate as a function of the signal-photon count rate when the signal is delayed with respect to the idler by one pulse period. The delay was achieved by inserting a fiber patch-cord of appropriate length in the signal path from the output of the filter to APD1. For two independent photon sources, each with a count rate $R_S \ll 1$, the "accidental" coincidence rate R_C is given by $R_C = R_S^2$, regardless of the photon statistics of the sources. This quadratic relation is plotted as the solid line in Fig. 4, which fits the delayed-coincidence data (triangles) very well. These measurements then show that while the fluorescence photons produced by the adjacent pump pulses are independent, those coming from the same pump pulse show a strong correlation, which is a signature of their nonclassical behavior.

In the second experiment, measurements were performed to demonstrate the nonclassicality test described in [13]. It can be shown that the inequality

$$R_C - R_C^{(a)} - 2\left(R_{S/2} - R_{S/2}^{(a)} + R_{I/2} - R_{I/2}^{(a)}\right) \leq 0 \quad (1)$$

is valid for two classical light sources, where R_C is the coincidence-count rate for the two sources, $R_C^{(a)}$ is the calculated "accidental" coincidence-count rate corresponding to the same photon-count rate for the two sources, $R_{S/2}$ and $R_{I/2}$ are the coincidence-count rates measured by passing the light from each of the two sources through a 50/50 splitter and detecting the two halves independently, and $R_{S/2}^{(a)}$ and $R_{I/2}^{(a)}$ are the calculated "accidental" coincidence-count rates in the 50/50 splitting measurements. When we substitute the experimental data, (1) yields $(64 \pm 9)10^{-6} \leq 0$, where the error is statistical. The inequality for classical sources is thus violated by over seven standard deviations.

In conclusion, we have demonstrated, for the first time to our knowledge, a source of quantum-correlated photon pairs that is based on FWM in a fiber near 1550 nm. We have also developed and tested a room-temperature coincidence detector for the photons in that window. The photon-pair detection rate ($\simeq 10^3$ coincidence counts/s) at present is limited by the electronics employed in our setup. In addition, we believe that the spectral filter used for rejecting the pump photons can be implemented with fiber Bragg gratings, making this source integrable with the existing fiber-optic infrastructure.

ACKNOWLEDGMENT

The authors would like to gratefully thank S. Endicter and M. Itzler from Epitaxx-JDS Uniphase for providing the APDs used in this experiment, and G. A. Barbosa for useful discussions.

REFERENCES

[1] C. H. Bennett and P. W. Shor, "Quantum information theory," *IEEE Trans. Info. Theory*, vol. 44, pp. 2724–2742, Oct. 1998.
[2] *J. Mod. Opt.*, vol. 48, no. 13, Nov. 2001.
[3] P. G. Kwiat, E. Waks, A. G. White, I. Appelbaum, and P. H. Eberhard, "Ultrabright source of polarization-entangled photons," *Phys. Rev. A*, vol. 60, pp. R773–R776, Aug. 1999.
[4] G. Bonfrate, V. Pruneri, P. G. Kazansky, P. Tapster, and J. G. Rarity, "Parametric fluorescence in periodically poled silica fibers," *Appl. Phys. Lett.*, vol. 75, pp. 2356–2358, Oct. 1999.
[5] S. Tanzilli, H. De Riedmatten, W. Tittel, H. Zbinden, P. Baldi, M. De Micheli, D. B. Ostrowsky, and N. Gisin, "Highly efficient photon-pair source using periodically poled lithium niobate waveguide," *Electron. Lett.*, vol. 37, Jan. 2001.
[6] C. E. Kuklewicz, E. Keskiner, F. N. C. Wong, and J. H. Shapiro, "A high-flux entanglement source based on a doubly-resonant optical parametric amplifier," *J. Opt. B: Quantum and Semiclass. Opt.*, vol. 4, June 2002.
[7] J. E. Sharping, M. Fiorentino, and P. Kumar, "Observation of twin-beam-type quantum correlation in optical fiber," *Opt. Lett.*, vol. 26, pp. 367–369, Mar. 2001.
[8] R. H. Stolen and J. E. Bjorkholm, "Parametric amplification and frequency conversion in optical fibers," *IEEE J. Quantum Electron*, vol. 18, pp. 1062–1072, July 1982.
[9] A. Lacaita, P. A. Francese, F. Zappa, and S. Cova, "Single-photon detection beyond 1 μm: performance of commercially available InGaAs/InP detectors," *Appl. Opt.*, vol. 35, pp. 2986–2996, June 1996.
[10] G. Ribordy, J.-D. Gautier, H. Zbinden, and N. Gisin, "Performance InGaAs/InP avalanche photodiodes as gated-mode photon counters," *Appl. Opt.*, vol. 37, pp. 2272–2277, Apr. 1998.
[11] J. G. Rarity, T. E. Wall, K. D. Ridley, P. C. M. Owens, and P. R. Tapster, "Single-photon counting for the 1300-1600-nm range by use of Peltier-cooled and passively quenced InGaAs avalanche photodiodes," *Appl. Opt.*, vol. 39, pp. 6746–6753, Dec. 2000.
[12] P. A. Hiskett, G. S. Buller, A. Y. Loudon, J. M. Smith, I. Gontijo, A. C. Walker, P. D. Townsend, and M. J. Robertson, "Performance and design of InGaAs/InP photodiodes for single-photon counting at 1.55 μm," *Appl. Opt.*, vol. 39, pp. 6818–6829, Dec. 2000.
[13] X. Y. Zou, L. J. Wang, and L. Mandel, "Violation of classical probability in parametric down-conversion," *Optical Communications*, vol. 84, pp. 351–354, Aug. 1991.